Cancer Imaging (2012) **12,** 423–436
DOI: 10.1102/1470-7330.2012.0038

CI

e-med
www.e-med.org.uk

ORIGINAL ARTICLE

Differentiation of glioblastoma multiforme from metastatic brain tumor using proton magnetic resonance spectroscopy, diffusion and perfusion metrics at 3 T

Ioannis Tsougos[a,*], Patricia Svolos[a,*], Evanthia Kousi[a], Konstantinos Fountas[b], Kyriaki Theodorou[a], Ioannis Fezoulidis[c], Eftychia Kapsalaki[c]

[a]Medical Physics Department, University of Thessaly, Biopolis, 41110 Larissa, Greece; [b]Department of Neurosurgery, University Hospital of Larissa, Biopolis, 41110 Larissa, Greece and [c]Department of Radiology, University Hospital of Larissa, Biopolis 41110, Larissa, Greece

Corresponding address: Dr Ioannis Tsougos, Medical Physics Department, University Hospital of Larissa, Biopolis, 41110 Larissa, Greece.
Email: tsougos@med.uth.gr

**These authors contributed equally.*

Date accepted for publication 31 July 2012

Abstract

Purpose: To assess the contribution of ^{1}H-magnetic resonance spectroscopy (^{1}H-MRS), diffusion-weighted imaging (DWI), diffusion tensor imaging (DTI) and dynamic susceptibility contrast-enhanced (DSCE) imaging metrics in the differentiation of glioblastomas from solitary metastasis, and particularly to clarify the controversial reports regarding the hypothesis that there should be a significant differentiation between the intratumoral and peritumoral areas. **Methods:** Conventional MR imaging, ^{1}H-MRS, DWI, DTI and DSCE MRI was performed on 49 patients (35 glioblastomas multiforme, 14 metastases) using a 3.0-T MR unit. Metabolite ratios, apparent diffusion coefficient (ADC), fractional anisotropy (FA) and relative cerebral blood volume (rCBV) were measured in the intratumoral and peritumoral regions of the lesions. Receiver-operating characteristic analysis was used to obtain the cut-off values for the parameters presenting a statistical difference between the two tumor groups. Furthermore, we investigated the potential effect of the region of interest (ROI) size on the quantification of diffusion properties in the intratumoral region of the lesions, by applying two different ROI methods. **Results:** Peritumoral *N*-acetylaspartate (NAA)/creatine (Cr), choline (Cho)/Cr, Cho/NAA and rCBV significantly differentiated glioblastomas from intracranial metastases. ADC and FA presented no significant difference between the two tumor groups. **Conclusions:** ^{1}H-MRS and dynamic susceptibility measurements in the peritumoral regions may definitely aid in the differentiation of glioblastomas and solitary metastases. The quantification of the diffusion properties in the intratumoral region is independent of the ROI size placed.

Keywords: *Spectroscopy; diffusion-weighted imaging; dynamic susceptibility contrast-enhanced imaging; glioblastoma; metastasis.*

Introduction

Primary glioblastoma multiforme (GBM) and intracranial metastases are the most commonly identified brain tumors in the adult population. Conventional magnetic resonance (MR) imaging of glioblastomas and solitary intracranial metastatic lesions may be indistinguishable, often displaying lack of differentiation between these two entities, as their imaging characteristics and contrast-enhancement patterns may be similar in many cases. Preoperative differentiation between these lesions may contribute to better treatment planning[1]. In the last years, advanced MR imaging techniques such as proton magnetic resonance spectroscopy (^{1}H-MRS), Diffusion-weighted imaging (DWI), diffusion tensor imaging (DTI) and dynamic susceptibility contrast-enhanced (DSCE)

This paper is available online at http://www.cancerimaging.org. In the event of a change in the URL address, please use the DOI provided to locate the paper.

MRI have provided information regarding the physiologic and metabolic characterization of brain tissue. MR imaging has shifted toward functional and molecular MR imaging, thus promising to improve MR specificity and provide an insight into the underlying biological characteristics of brain tumors[2,3]. In vivo ^{1}H-MRS provides a metabolic profile of brain tumors, measuring specific amino acids such as *N*-acetylaspartate (NAA), choline (Cho), creatine (Cr), lipids (Lip), and lactate (Lac), and their relative ratios[1]. In most brain tumors, a non-specific pathologic spectrum consisting of increased Cho/Cr and decreased NAA/Cr ratios is detected, indicating loss of neuronal integrity and increased myelin turnover, respectively[4]. Presence of lactate and lipid peaks are usually consistent with aggressive tumors, reflecting increased anaerobic metabolism and cellular necrosis, respectively[1,2,5–12]. Diffusion-weighted imaging provides information about the diffusion properties of water molecules in different cerebral regions. The apparent diffusion coefficient (ADC) is an index that gives a rough evaluation of water diffusion in a certain region, considering diffusion as an isotropic process. However, studies have shown that ADC is rotationally dependent; pointing out that water diffusion is restricted or facilitated toward certain directions[13,14]. Diffusion tensor imaging represents a further development of DWI, taking into account the directionality of water diffusion in a certain voxel due to the microstructure of the underlying tissue. Fractional anisotropy (FA) is a quantitative index reflecting the magnitude of the orientated water diffusion, and is considered to be a parameter associated with the architecture and integrity of white matter in the brain parenchyma[13–15].

DSCE MRI enables non-invasive qualitative and quantitative measurements of tumor vascularity[1,16]. Relative cerebral blood volume (rCBV) maps derived from DSCE MRI can be used to quantify areas of neovascular proliferation, which has been reported to be one of the most important factors responsible for the histopathological type of tumors, rendering DSCE MRI an important technique for characterizing intracranial neoplasms[3,5].

All the aforementioned MR imaging methods have promised to distinguish glioblastomas from solitary metastatic brain tumors. Regarding the intratumoral part of these lesions, ^{1}H-MRS initially sought to differentiate between the two lesions, identifying a high degree of lipid signal in metastatic tumors compared with glioblastomas. However, this was not supported by the majority of the published data[8–11]. Therefore, interest was focused on the peritumoral edema. The hypothesis posits that glioblastomas are infiltrative lesions, thus pathologic tissues may be present in the surrounding white matter while metastatic lesions are not. Therefore, the surrounding edema of metastases is considered to be purely vasogenic, whereas around glioblastomas there should be a combination of vasogenic edema and infiltrating tumor cells along the perivascular spaces. Based on these peritumoral characteristics, ^{1}H-MRS studies have shown a significant distinction between the two lesions[1,17].

Regarding diffusion, theoretically water diffusion around glioblastomas is expected to be facilitated by tumor infiltrations, resulting in higher ADC values and lower FA, whereas around non-infiltrating metastases both indices should reach the normal values. However, the results from DWI and DTI metrics, both for intratumoral and peritumoral measurements, have been controversial[1,18–26].

Moreover, similarly to ^{1}H-MRS studies, it has been demonstrated that intratumoral rCBV measurements do not contribute significantly to differentiation, whereas peritumoral measurements have been proved to be significantly important, reflecting the difference in pathophysiologic mechanisms between glioblastomas and intracranial metastatic tumors[1,8,16].

The objective of the present study was to assess the overall contribution of ^{1}H-MRS, DWI/DTI, and DSCE MRI metrics in the differentiation of glioblastomas from solitary metastasis, and particularly to evaluate the hypothesis that there should be a significant differentiation between the intratumoral and peritumoral areas.

Materials and methods

Patients

Our prospective clinical study was approved by the hospital institutional review board. Patients with a solitary brain tumor with conventional MR imaging characteristics compatible with a glioblastoma or a metastatic lesion were included in our study. Our inclusion criteria sought adult, cooperative patients with a solitary, inhomogeneous, contrast-enhancing brain lesion. Exclusion criteria were children, multiple lesions, prior surgery, and chemotherapy or radiation therapy. Written informed consent was obtained from all patients included in the study. ^{1}H-MRS, DWI, DTI and DSCE MRI were performed on 49 patients (aged 32–73 years) with a solitary brain tumor (35 GBM and 14 metastases). The metastases group consisted of 6 lung and 8 breast primary tumors. The diagnosis (after the analysis of the neuroradiologist and medical physicist) was suggested before surgery. All patients underwent total or partial surgical resection of their lesions with the aid of a frameless neuro-navigational system in our institution. All surgical procedures were performed within a month of the neuroimaging analysis. A histopathological diagnosis was obtained in all cases, and was finally compared with our imaging results.

Conventional MR imaging, ^{1}H-MRS, DWI, DTI and DSCE examination protocols

The study was performed on a 3-T MR whole-body scanner (Signa HDx; GE Healthcare, Waukesha, WI, USA)

applying a standardized MRI, ^{1}H-MRS, DWI, DTI and DSCE examination patient protocol, using a 4-channel birdcage and an 8-channel phased-array head coil. Conventional MRI protocol included pre-contrast sagittal and transverse T1-weighted fast spin-echo (FSE) (repetition time (TR)/echo time (TE) 700 ms/9.3 ms), transverse T2-weighted FSE (TR/TE 2640 ms/102 ms), coronal T2-weighted FSE (TR/TE 2920 ms/102 ms), and T2-weighted fluid attenuation inversion recovery (FLAIR) (TR/TE 8500 ms/130 ms). Diffusion-weighted MR imaging was performed via a single-shot, spin-echo, echo planar sequence with b value of 0 and 1000 s/mm^2.

To accurately quantify ADC in a region of interest (ROI) high b values may be used, because parameter b is directly correlated with the diffusion sensitization. However, the b values selected in this study are in accordance with the values most commonly used in the literature. Therefore, one who is not familiar to diffusion metrics can directly compare and evaluate our results with those previously reported.

Post-contrast isotropic 3-dimensional spoiled gradient echo (3D-SPGR, TR/TE 6.9 ms/2.1 ms, 12° flip angle, 240×240 mm^2 field of view (FOV), 136 slices of 1 mm thickness) and T1-weighted FSE (TR/TE 700 ms/9.3 ms) axial images were also obtained.

^{1}H-MRS imaging was performed using PROton Brain Exam (PROBE) 2-dimensional multivoxel (2D-chemical shift imaging (CSI)) spectroscopy before contrast administration to avoid signal disturbance. Data were acquired using Point-RESolved Spectroscopy (PRESS) pulse sequence with phase-encoding gradients in two directions, automatic shimming and Gaussian water suppression. Measurement parameters used in 2D-CSI were 1000/144 ms (TR/TE), 16×16 phase-encoding steps and 10-mm section thickness, and the FOV size was adjusted to each patient's brain anatomy.

DTI was performed prior to contrast media injection, in the axial plane with single-shot spin-echo echo planar imaging with the following parameters: TR/TE 8000 ms/89.8 ms, gradients applied in 15 nonlinear directions, $b = 0$ and 1000 s/mm^2, FOV = 24 mm, slice thickness = 40 mm with gap = 1 mm and NEX = 1.

The DSCE MR images were acquired with a single-shot gradient echo echo planar imaging sequence (TR/TE 2000 ms/20.7 ms, flip angle 60°, FOV = 24 mm, thickness = 5 mm with gap = 0 mm, NEX = 1) during the first pass of bolus of contrast material at a dose of >0.4 mmol/kg body weight. The section thickness and location of the perfusion-weighted MR data set were determined by using the axial T1-weighted images after contrast injection to locate the lesion and axial T2-weighted images to locate the peritumoral T2 signal abnormality.

The overall evaluation of ^{1}H-MRS, DWI/DTI and perfusion-weighted imaging, as well as the analysis and decision making per patient, is a quite time-consuming process which, in some cases, may definitely exceed the available time per patient in terms of clinical routine. The duration of the whole procedure was approximately 1 h.

Data post-processing

^{1}H-MRS

Spectra for each patient were acquired from the intratumoral, peritumoral and contralateral regions (Figs. 1 and 2). The contralateral normal area (cNA) was used as the control spectrum. A rectangular ROI was localized by using the transverse T2-weighted FLAIR or T2-weighted FSE, sagittal T1-weighted FSE and coronal T2-weighted FSE imaging sequences. In vivo 2D-CSI spectroscopic data analysis and calculation of metabolite ratios were performed on an Advantage Linux workstation using the Functool software (GE Healthcare). Post-processing of the raw spectral data included baseline correction, frequency inversion and phase shift. Gaussian curves were fitted to NAA, Cho, Cr, lipid and lactate peaks for determination of peak area. Finally, metabolite ratios of NAA/Cr, Cho/Cr, Cho/NAA and (Lip+Lac)/Cr were calculated from the area under each metabolite peak for each ROI separately.

It should be noted that the spectroscopic examination was performed by an MR physicist, as this technique requires the adjustment of several pre-acquisition parameters in order to ensure signal quality. However, the metabolic information provided is highly correlated with the underlying pathophysiology. Hence, the overall evaluation of the spectroscopic findings in combination with the imaging characteristics of the tumor under study requires the co-operation of both the radiologist and the MR physicist.

DWI and DTI

ADC maps were acquired from isotropic DWI and FA maps were acquired from DTI. All measurements were performed on the Advantage Linux workstation using the Functool software. ROIs were placed manually in the intratumoral, peritumoral and contralateral region of each lesion using T2-weighted, T2-weighted FLAIR and T1-weighted post-contrast images as reference images to guide the accurate ROI placement. In the intratumoral region two different ROI methods were applied. A large ROI was placed covering as much as possible the interior border of the tumor, with a diameter ranging from 118 to 990 mm^2 depending on the tumor size. A number of smaller ROIs were placed inside this ROI (we called this the "revolver technique", see Fig. 3), with a diameter ranging from 10 to 62 mm^2. The aim was to investigate the potential effect the ROI placement might have on the measured ADC and FA values and to evaluate their eventual differences. Inside the tumor region, ROIs were placed in the solid parts that exhibited contrast enhancement, while in the peritumoral area they were placed on

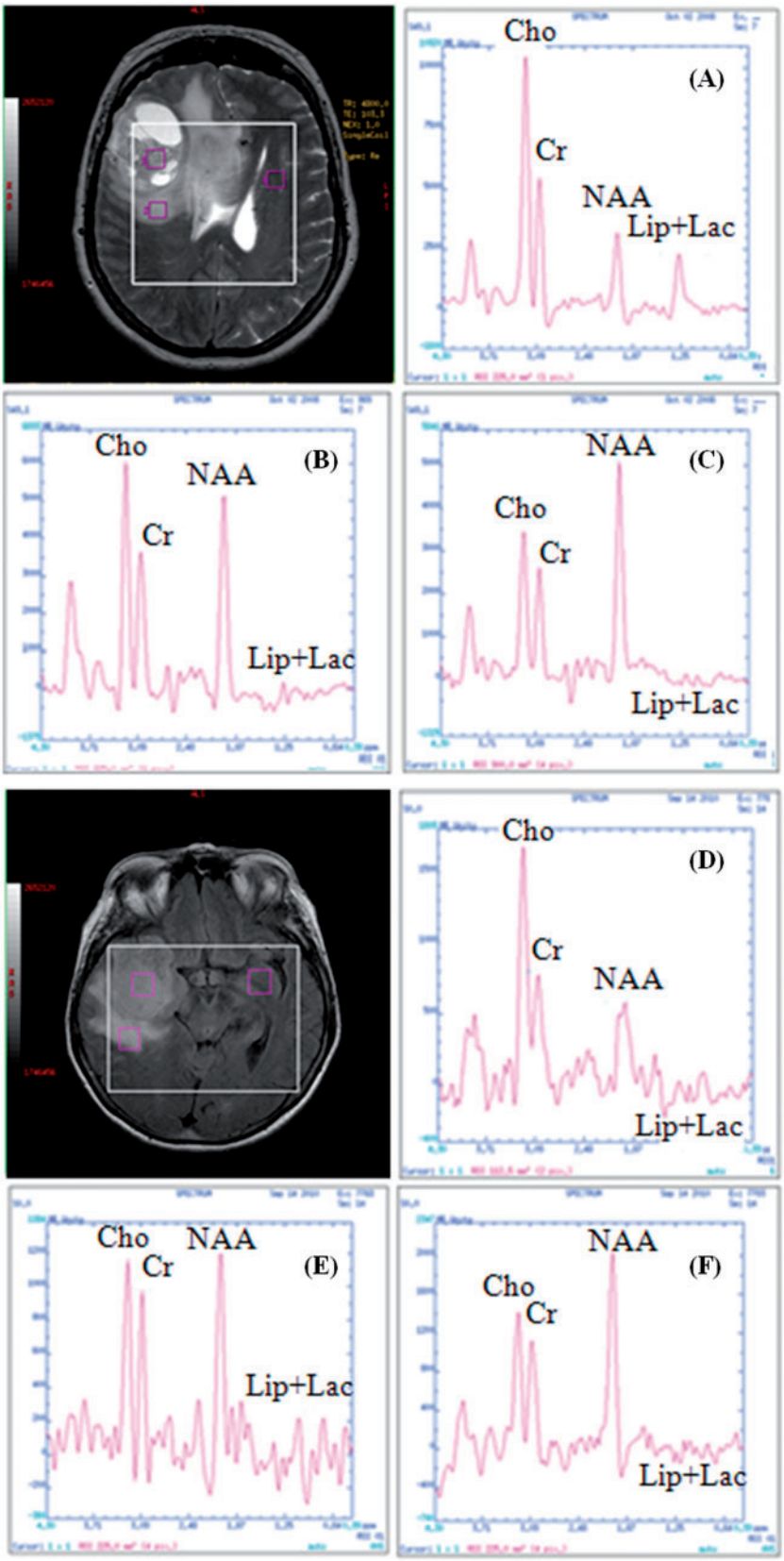

Figure 1 **Localizing axial T2-weighted fast spin-echo (T2-FSE) magnetic resonance (MR) image of a 50-year-old woman (upper) and T2-weighted fluid-attenuated inversion recovery (T2-FLAIR) MR image of a 67-year-old man (lower) with glioblastoma. The voxels of interest, with their corresponding spectra, are illustrated: intratumoral (A, D), peritumoral (B, E) and contralateral normal area (C, F).**

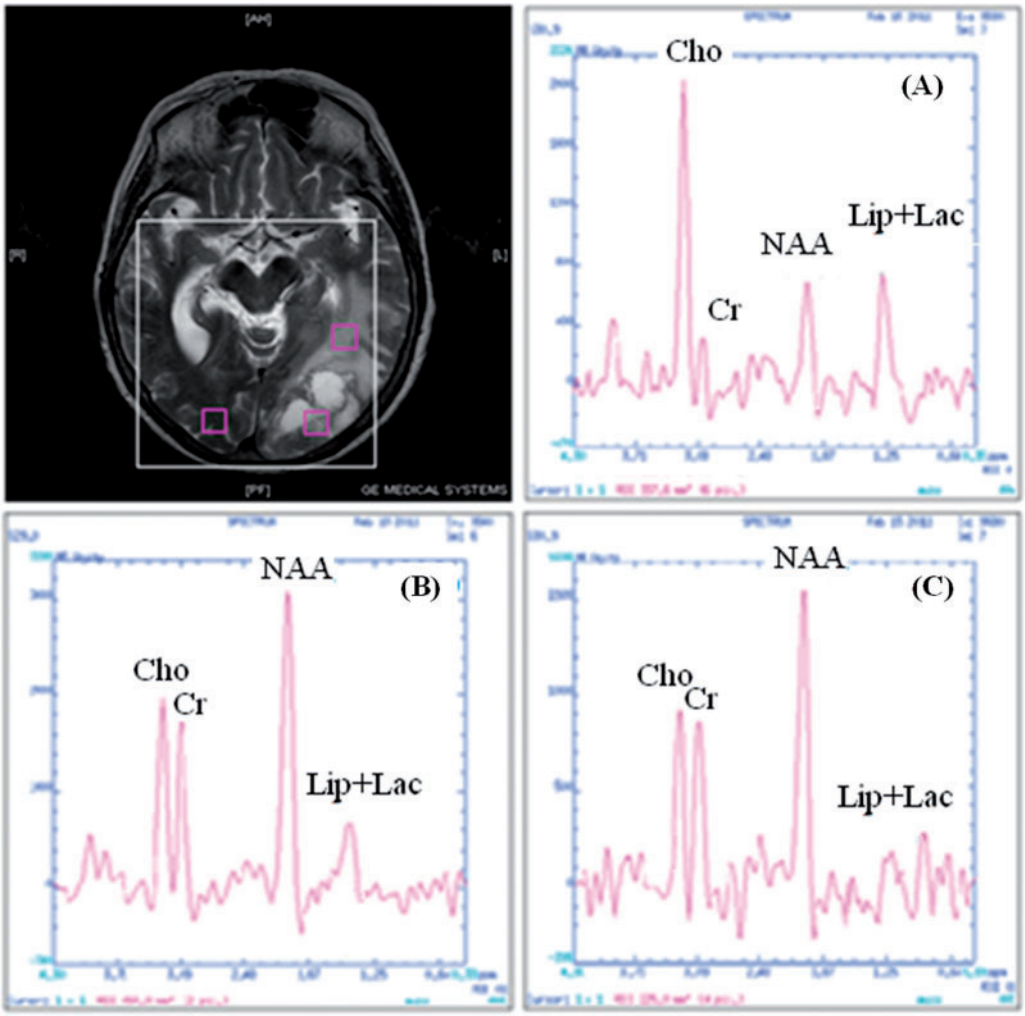

Figure 2 **Localizing axial T2-FSE MR image of a 58-year-old man with intracranial metastases from lung carcinoma. The voxels of interest, with their corresponding spectra, are illustrated: intratumoral (A), peritumoral (B) and contralateral normal area (C).**

the border between the tumor lesion and its surroundings, as shown on T2-weighted and T1-weighted post-contrast images.

DSCE MRI

For DSCE MRI the data were processed on the GE workstation with the Functool software. T2*-weighted images were firstly corrected for motion artifacts with Brainstat software. The rCBV map (approximated by using the negative enhancement integral) was then overlaid on the T2*-weighted image.

The rCBV measurements were calculated from ROIs, which were placed in regions of the highest perfusion as seen on the rCBV color overlay maps. Six to ten ROIs, ranging in size from 30 to 60 mm^2 each, were placed in the tumor to record the maximal rCBV value. Inside the tumor the placement of ROIs was carefully performed to avoid large vessels, based on the combined information from T1-weighted image after contrast enhancement, T2-weighted FSE image, and T2*-weighted image. The peritumoral region was defined to be within 1 cm outside the enhancing tumor margin with maximum rCBV (Fig. 3D). The rCBV values were measured in 3–6 ROIs within the peritumoral region. For comparison, rCBV was also measured in a distant area of the ipsilateral normal-appearing parenchyma to ensure rCBV increment from the intratumoral and peritumoral regions.

Finally, the rCBV ratio was calculated by dividing the rCBV value either from the intratumoral or peritumoral region, outlined above, with the rCBV value from the contralateral ROI.

Regardless of the MR technique performed, inside the region of tumor tissue under study, obvious necrosis, cyst, hemorrhage, edema, calcification and normal-appearing brain tissue were excluded from the voxel or ROI whenever possible, in order to avoid false lesion estimation. Voxel and ROI placement was performed without knowledge of the histological information.

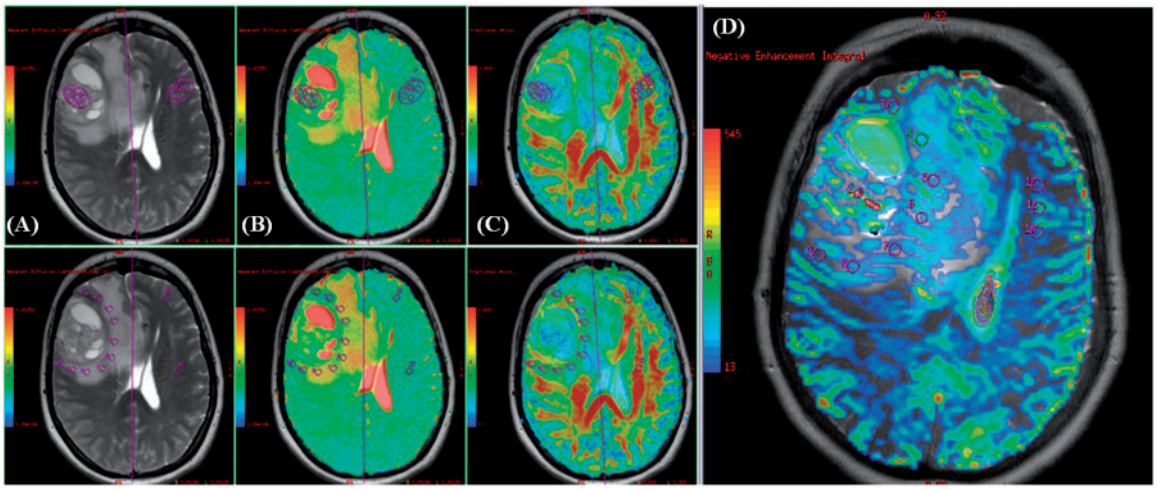

Figure 3 **Diffusion and perfusion measurements. Localizing T2-FSE MR image with superimposed apparent diffusion coefficient (ADC), fractional anisotropy (FA) and relative cerebral blood volume (rCBV) color maps, of a 50-year-old woman with glioblastoma multiforme. ROI placement in different tumor regions and the contralateral normal area. Upper row: intratumoral region ("revolver technique"); lower row: peritumoral region. ROIs are placed on T2-weighted reference images (column A), on ADC maps (column B) and on FA maps (column C) and on rCBV maps (column D).**

The ADC, FA and rCBV measurements were performed by two separate readers (radiologist and MR physicist).

Statistical analysis

We grouped the patients according to tumor type (glioblastoma/metastasis). Statistical analysis was performed using the SPSS (version 13) statistical software package. Parameter values were expressed as mean ± standard deviation (SD). The Mann–Whitney test was used to explore parameter relationships and compare ^{1}H-MRS, perfusion, diffusion and anisotropy values between glioblastomas and metastases. To determine the combination of the most discriminative parameters and identify their optimal cut-off values, receiver-operating characteristic (ROC) curve analysis based on logistic regression models was performed. The efficacies of the parameters were assessed in terms of sensitivity and specificity. *P* values of less than 0.05 were considered statistically significant.

Results

^{1}H-MRS

The metabolic ratio values of NAA/Cr, Cho/Cr, Cho/NAA and Lip+Lac/Cr, measured for the intratumoral regions were 1.19 ± 0.48, 3.13 ± 1.28, 3.08 ± 1.87 and 3.39 ± 3.76, respectively, for glioblastomas and 1.67 ± 0.83, 4.56 ± 2.34, 2.76 ± 2.59 and 7.18 ± 11.09, respectively, for metastases.

For the peritumoral regions, the metabolic ratio values for NAA/Cr, Cho/Cr, Cho/NAA and Lip+Lac/Cr were 1.46 ± 0.50, 1.66 ± 0.56, 1.28 ± 0.66 and 0.68 ± 0.47 for glioblastomas, and 1.91 ± 0.34, 1.29 ± 0.27, 0.69 ± 0.16 and 0.62 ± 0.31 for metastases. In addition, metabolic ratios were calculated from the cNA, which is important to ensure metabolic ratio abnormality from the intratumoral and the peritumoral regions.

The mean ± SD of the metabolite ratios within the tumor and the peritumoral area as well as the cNA of glioblastomas and metastases are summarized in Table 1.

Intratumoral region

All computed metabolite ratios of the intratumoral regions of glioblastomas and metastases were statistically different from those of the cNA, revealing a distinct differentiation of the two lesion types from the normal brain parenchyma, with the exception of NAA/Cr of metastases, which was calculated as marginally close to the cNA levels.

Comparing the metabolite ratios between glioblastomas and metastases intratumorally, no statistically significant difference was observed, revealing the lack of differentiation ability of spectroscopic imaging in the intratumoral region (Table 1). Nevertheless, a trend of intratumoral Cho/Cr ratio toward higher values for metastases was observed when compared with that of glioblastomas. However, because of the wide corresponding SDs this tendency was not statistically confirmed.

Peritumoral region

The calculated peritumoral metabolite ratio values of glioblastomas were statistically different from the corresponding control values of the normal brain

Table 1 **Parameter mean values with their corresponding standard deviation, and comparison results in the intratumoral, peritumoral and contralateral normal area**

Metrics	Intratumoral			Peritumoral			Contralateral normal area	
	GBM	Metastasis	*P*	GBM	Metastasis	*P*	GBM	Metastasis
NAA/Cr	1.19 ± 0.48*	1.67 ± 0.83	0.17	1.46 ± 0.50*	1.91 ± 0.34	0.01**	1.79 ± 0.44	1.97 ± 0.38
Cho/Cr	3.13 ± 1.28*	4.56 ± 2.34*	0.17	1.66 ± 0.56*	1.29 ± 0.27	0.05**	1.30 ± 0.36	1.09 ± 0.23
Cho/NAA	3.08 ± 1.87*	2.76 ± 2.59*	0.21	1.28 ± 0.66*	0.69 ± 0.16	<0.01**	0.81 ± 0.51	0.57 ± 0.13
Lip+Lac	3.39 ± 3.76*	7.18 ± 11.09*	0.12	0.68 ± 0.47*	0.62 ± 0.31	0.973	0.47 ± 0.27	0.49 ± 0.14
ADC	1.279 ± 0.463*	1.176 ± 0.524*	0.185	1.054 ± 0.220*	1.105 ± 0.148*	0.232	0.973 ± 0.225	0.858 ± 0.109
FA	0.147 ± 0.065*	0.119 ± 0.047*	0.249	0.291 ± 0.075	0.261 ± 0.063	0.293	0.299 ± 0.107	0.321 ± 0.072
rCBV	11.49 ± 6.33*	10.80 ± 5.13*	0.98	1.68 ± 0.59*	1.06 ± 0.38	0.02**	1.13 ± 0.36	0.96 ± 0.19

NAA, *N*-acetylaspartate; Cho, choline; Cr, creatine; Lip, lipids; Lac, lactate; ADC, apparent diffusion coefficient; FA, fractional anisotropy; rCBV, relative cerebral blood volume; GBM, glioblastoma multiforme.
P values represent Mann–Whitney *U* test for NAA/Cr, Cho/Cr, Cho/NAA, (Lip+Lac)/Cr, ADC, FA and rCBV ratios for both intratumoral and peritumoral areas between glioblastomas and metastases.
Contralateral normal area for metabolite ratios, FA values and ADC values has been considered the contralateral side of the tumor, whereas for rCBV ratio the contralateral normal area has been considered a distant area (>2 cm) from the tumor.
*Parameter significant difference between the metabolite ratios, diffusion and perfusion values from the corresponding contralateral normal area values ($P<0.05$).
**Parameter significant difference between glioblastoma and intracranial metastases.

parenchyma. On the contrary, the metabolic ratio values from the peritumoral region of metastases were very close to the corresponding values of the cNA (Table 1).

Especially for glioblastomas, the peritumoral area consisted of two spectral patterns. The first pattern (Fig. 1B) revealed high Cho and low NAA peaks (70% of glioblastoma cases), whereas the second (Fig. 1E) revealed a low NAA peak with no distinct evidence of Cho elevation. The peritumoral region of intracranial metastases appeared with normal metabolic pattern consistent with that of the cNA (Fig. 2B).

Hence, comparing the metabolite ratios in the peritumoral ROI between the two lesion types, NAA/Cr, Cho/Cr and Cho/NAA ratios were significantly different ($P<0.05$) (Table 1), reflecting the different pathophysiologic findings on the periphery of the two lesions. However, an overlapping of these metabolite ratios between the tumor groups under study still exists, even in the case of Cho/NAA, which shows the best discrimination ability ($P<0.01$) as illustrated in Fig. 4.

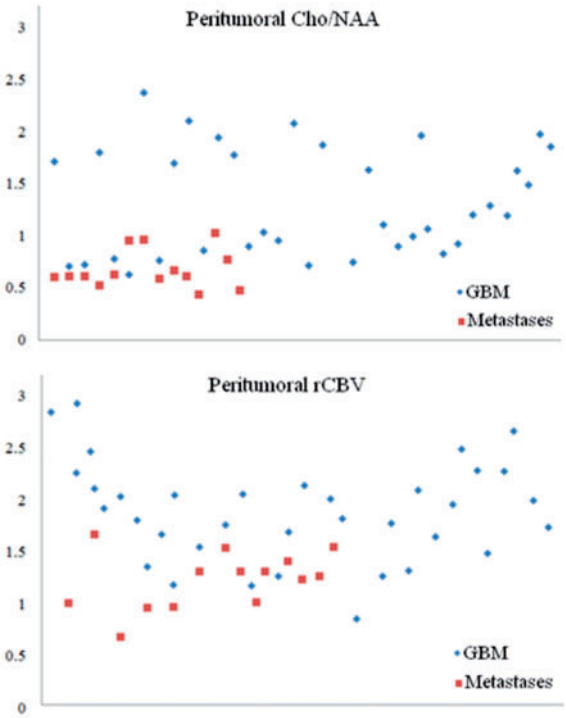

Figure 4 **Scatter plots of the main discriminators (choline/*N*-acetylaspartate and rCBV) in the peritumoral region.**

DWI and DTI

The mean values ± SD of ADC and FA were calculated for the intratumoral and peritumoral region as well as for the cNA area. All measurements are summarized in Table 1.

Intratumoral region

Specifically, in the intratumoral region the mean value ± SD of the smaller ROIs was computed for each parameter and compared with the obtained value from the larger ROI (Table 2). In the intratumoral region of glioblastomas and metastatic lesions, both ADC and FA were significantly different ($P<0.05$) from the corresponding contralateral normal values (Table 1).

In the intratumoral region of glioblastomas, the mean ADC and FA values were $ADC_{(GBM)} = 1.279 \pm 0.463\,mm^2/s$ and $FA_{(GBM)} = 0.147 \pm 0.065$, whereas in metastatic tumors the mean values were $ADC_{(Meta)} = 1.176 \pm 0.524\,mm^2/s$ and $FA_{(Meta)} = 0.119 \pm 0.047$. Comparing the ADC and FA values obtained from the intratumoral region of both tumor groups, no statistically significant differences were observed ($P>0.05$).

Table 2 **Comparison of ADC and FA values between the large and small ROIs in the intratumoral region of glioblastomas and metastatic tumors**

	Intratumoral region			
	GBM		Metastasis	
	ADC	FA	ADC	FA
Large ROI	1.272 ± 0.452	0.152 ± 0.062	1.189 ± 0.530	0.122 ± 0.050
Small ROI	1.279 ± 0.463	0.147 ± 0.065	1.176 ± 0.524	0.119 ± 0.047
P value	0.882	0.763	0.931	0.792

Peritumoral region

Concerning the peritumoral area of both glioblastomas and metastatic tumors, the ADC differed significantly in comparison with the obtained control values.

Around glioblastomas the mean values of ADC and FA were $ADC_{(GBM)} = 1.054 \pm 0.220\,mm^2/s$ and $FA_{(GBM)} = 0.291 \pm 0.075$; around metastatic tumors the mean values obtained were $ADC_{(Meta)} = 1.105 \pm 0.148\,mm^2/s$ and $FA_{(Meta)} = 0.261 \pm 0.063$. However, ADC and FA values measured in the peritumoral region of glioblastomas and metastases did not enable the differentiation between the two tumor groups, as the observed differences did not reach statistical significance.

The two different ROI methods applied in the intratumoral region of the tumor groups investigated showed no statistical difference. The ADC and FA value obtained from the larger ROI was similar ($P > 0.05$) compared with the mean value of the smaller ROIs for each parameter. The results are summarized in Table 2.

DSCE imaging

The rCBV ratio measurements were performed for the intratumoral and peritumoral regions of the two tumor groups. The mean ± SD and the comparison results of rCBV ratio in each ROI, as well as the rCBV ratio values from distant normal-appearing areas of the tumors, are shown in Table 1.

Intratumoral region

In the intratumoral region, the rCBV ratio values were $rCBV_{(GBM)} = 11.49 \pm 6.33$ for glioblastomas and $rCBV_{(Meta)} = 10.80 \pm 5.13$ for metastases. The intratumoral rCBV ratios of metastases and glioblastomas were significantly higher ($P < 0.05$) than the corresponding rCBV value of the normal-appearing area (Table 1). Comparing the rCBV ratios of the intratumoral area, between the two tumor types no statistically significant difference was revealed.

Peritumoral region

Around glioblastomas rCBV ratio values were $rCBV_{(GBM)} = 1.68 \pm 0.59$, whereas around metastases the rCBV ratio was $rCBV_{(Meta)} = 1.06 \pm 0.38$. The computed rCBV ratio of the peritumoral region of glioblastomas was significantly different ($P < 0.05$) from those of the control area, whereas the peritumoral rCBV ratio values of intracranial metastases did not differ from the corresponding control values. Hence the rCBV ratio from the peritumoral ROI proved to be a strong index ($P < 0.05$) in differentiating between glioblastomas and intracranial metastases (Table 1), despite the slight overlapping of the rCBV values observed (Fig. 4).

ROC curve analysis

To acquire cut-off values that could differentiate GBM from intracranial metastasis, ROC curve analysis was implemented.

For the peritumoral region only, among all the techniques applied the optimal cut-off values that were able to differentiate GBMs from intracranial metastases are NAA/Cr = 1.50, Cho/Cr = 1.40 and Cho/NAA = 1.10, and rCBV = 1.70 (Fig. 5).

The resulting sensitivity and specificity of the cut-off values are shown in Table 3. The area under the ROC curves revealed that these four ratios proved to be statistically powerful in differentiating the two tumor groups. The specificity of the peritumoral rCBV ratio proved to be superior to those of NAA/Cr, Cho/Cr and Cho/NAA ratios, while Cho/Cr achieved the highest sensitivity.

Discussion

Conventional MRI often poses difficulties in the differentiation of glioblastomas and solitary brain metastases, as they both demonstrate similar imaging characteristics and contrast-enhanced patterns. Preoperative distinction between these tumors is important for their surgical approach and therapeutic processes, which could be completely different[8]. Advanced MRI techniques such as ^{1}H-MRS, DWI, DTI and DSCE MRI are incorporated in conventional clinical MRI routine, providing physiologic and metabolic information, which may significantly contribute in tumor differentiation preoperatively.

Spectroscopy

NAA is generally recognized as a marker of functional neurons and their appendages despite of the fact that its function is not exactly known. Damage or destruction of

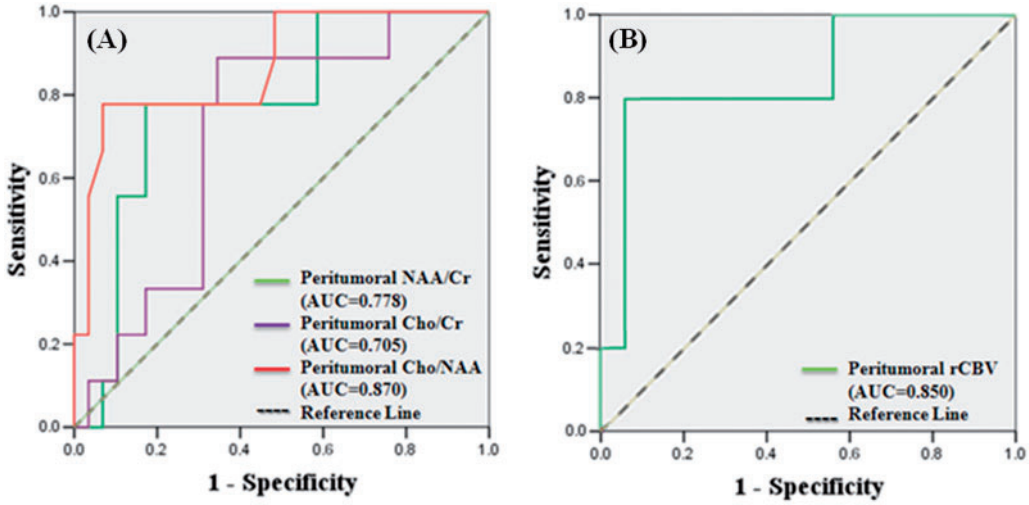

Figure 5 **(A) Receiver-operating characteristic (ROC) curves of peritumoral *N*-acetylaspartate (NAA)/creatine (Cr), choline (Cho)/Cr and Cho/NAA in differentiating glioblastomas multiforme (GBM) from intracranial metastases. (B) ROC curve of peritumoral rCBV in differentiating GBM from intracranial metastases.**

Table 3 **Measures of sensitivity and specificity by using NAA/Cr, Cho/Cr, Cho/NAA and rCBV ratios in the peritumoral ROI in discrimination of GBM from intracranial metastases**

Metabolite ratios	Cut-off value	Sensitivity (%)	Specificity (%)	AUC
NAA/Cr	1.50	78	82	0.778
Cho/Cr	1.40	89	62	0.705
Cho/NAA	1.10	78	93	0.870
rCBV ratio	1.70	80	94	0.850

AUC, area under the curve.

normal brain tissue by any destructive, degenerative or infiltrative process causes marked NAA reduction[10]. Both GBM and metastatic lesions cause normal brain destruction, therefore NAA is markedly reduced.

Intratumoral region

In our study, no statistically significant difference was observed in the metabolite ratio values between glioblastomas and metastases from the intratumoral region, which is in agreement with most previously reported findings[1,11,17]. In particular, we found a trend toward higher intratumoral Cho/Cr levels in metastases compared with GBMs (4.56 ± 2.34 and 3.13 ± 1.28, respectively), which was proved statistically non-significant. Several investigators report increased Cho/Cr ratio in metastatic lesions in comparison with GBMs in a statistically significant manner. Nevertheless, we consider that with an increase of our metastatic tumor sample this result will probably be statistically confirmed. Similarly, we found higher intratumoral NAA/Cr levels for metastases than for glioblastomas (1.67 ± 0.83 and 1.19 ± 0.48, respectively) but without statistical significance ($P = 0.17$). This may be attributed to the fact the metastatic lesions present lower concentrations of Cr, producing a higher Cho/Cr and NAA/Cr ratios.

On the other hand, in a limited series of nine primary and metastatic tumors, Bruhn et al. observed high Cho levels within the enhancing tumor, which did not allow differentiation between the two tumor types[27]. These conflicting results may be due to the differences in the intratumoral ROIs selected for analysis and the intrinsic heterogeneity of tumors.

Peritumoral region

As intratumoral heterogeneity may further complicate the selection of a voxel of interest, the peritumoral region may provide more reliable and reproducible results due to its relative homogeneity. In the present study, the metabolite ratios of NAA/Cr, Cho/Cr and Cho/NAA extracted from the peritumoral area were significantly different among glioblastomas and metastases. This difference in the peritumoral area can in part be explained by the difference in pathophysiology, where molecular mechanisms including abnormalities of tumor endothelium, vascular endothelial growth factor, and leukotriene synthase play a role[28]. Because of their infiltrative nature, peritumoral edema of high-grade gliomas represents a combination of vasogenic edema and neoplastic cell infiltration[2,5,28,29]. On the other hand, peritumoral edema of intracranial metastases is purely vasogenic because of increased extracellular water from the leakage of plasma fluid from altered tumor capillaries, but no tumor cells are present[2,5]. Our finding that Cho/Cr and Cho/NAA ratios in the peritumoral area of glioblastomas were significantly higher than those of metastases is consistent with previous observations[17,28–34]. However, Chiang et al. and Law et al. reported that

there was no significant difference in peritumoral NAA/Cr between the high-grade gliomas and metastases[1,8].

Taking this fact into account, it has to be stated that in 30% of our glioblastoma cases the peritumoral spectroscopic findings were marginally close to normal levels (Fig. 1E). In accordance with Chernov et al., it is possible to suspect that lipids and lactate, diffused from tumors with highly necrotic core as glioblastomas, make an important contribution to the depression of the neuronal function in the peritumoral brain tissue[35]. Alternatively, lipid-producing neoplasms may concurrently secrete other metabolites with a depressive effect on neurons of the surrounding brain. Several studies have reported that the presence of lipids in glioblastomas and metastases are due to areas of necrosis. However, Opstad et al. speculated that although sharing common lipid profiles, in glioblastomas and metastases lipid signal arises from different origins such as pure tumor necrosis for infiltrative tumor cells, and there is less necrosis combined with lipid membrane structure for migratory tumor cells, which might be a possible explanation for the lower peritumoral NAA/Cr on GBMs[30].

In our study, peritumoral NAA/Cr, Cho/Cr and Cho/NAA ratios achieved sensitivities of 78%, 89% and 78%, respectively, while NAA/Cr and Cho/NAA reached high specificity of 82% and 93%, respectively, in differentiating glioblastomas from metastases. The high specificity of peritumoral NAA/Cr and Cho/NAA ratios means that false-positive rates are low and the true-negative rates correspondingly high. In other words, most of the GBM cases will be correctly classified using these two ratio parameters. In addition, the corresponding area-under-the-curve values using peritumoral NAA/Cr and Cho/NAA ratios indicate that peritumoral NAA/Cr and Cho/NAA can be useful in discriminating glioblastomas from metastases. On the other hand, Cho/Cr reached a rather low specificity result (62%), which can be explained by the fact that some glioblastomas may not exhibit the tumoral pattern (high Cho level) to their perilesional area, as we observed in 30% of our cases (Fig. 1E).

It has to be mentioned that in this study, spectral measurements were performed using 2D-CSI in order to simultaneously sample the entire tumor, the peritumoral region and cNA, increasing the likelihood of demonstrating the most metabolically active portion of the tumor[8]. Nevertheless, since the signal in 2D-CSI is spatially encoded by a finite number of phase-encoding steps, the spatial origin of the signal does not generally coincide with the rectangular shape of the voxel in the spectroscopic grid. The signal of the voxel of interest may be contaminated with signals from other voxels, due to data reconstruction by the application of Fourier transform[28]. This phenomenon is referred to as voxel "bleeding" and should be considered as a limitation of this technique, because signal intensities obtained from voxels located on the edge of the tumor may be influenced by each other, and the values of the relative signal intensities in the peritumoral region may be distorted by strong resonances originating from the tumor.

Diffusion and anisotropy metrics

The intratumoral ADC and FA values obtained from the larger ROI as well as the number of smaller ROIs for both glioblastomas and metastases showed no statistical differences. The mean value from the smaller ROIs was similar to the one of the larger ROI for both parameters, indicating that water diffusion and anisotropy inside the solid area of a lesion might be independent of the ROI size placed. Therefore, it seems that placing a single ROI inside the intratumoral region can sufficiently describe the diffusion properties of this area.

Intratumoral region

In the present study the ADC and FA values measured in the intratumoral region of both tumor groups were significantly different to those in the cNA; nevertheless, there was no statistically significant differentiation between the two lesion types. A possible explanation for these findings is that because GBMs as well as metastatic lesions show tumor heterogeneities with necrotic and cystic regions, the diffusion of water molecules is facilitated and is considered to be more isotropic in comparison with the diffusion in normal areas. Therefore, inside these lesions the directionality of water diffusion is reduced, a process reflected as a relative decrease in FA values intratumorally compared with the FA values of the contralateral normal side[21,36–40]. Hence it is concluded that ADC and FA values of the intratumoral regions could not serve as predictive indices in the differentiation of these two tumor types, in accordance with previous studies[21–25].

However, based solely on the mean values and the corresponding SDs of the parameters as shown in Fig. 6B, the mean value of FA in glioblastomas is higher than in metastases, indicating roughly that FA might be a more appropriate index to quantify the diffusion properties in the intratumoral region of these two groups. The higher FA of glioblastomas in the present study may be attributed to the fact that glioblastomas present higher cellularity in the solid part of their lesion than do brain metastases[41,42]. Whether FA is positively or negatively correlated with tumor cell density and vascularity, and whether it can be used to assess tumor grading, is under wide dispute. Kinoshita et al. reported a positive correlation of FA with higher tumor cell density, and this correlation is still controversial[43]. Beppu et al. showed a linear increase of FA values and cell density, while Stadlbauer et al. showed that FA values decrease as cell density increases[37,44,45]. A possible reason for these conflicting reports could be the different tumor regions studied[46].

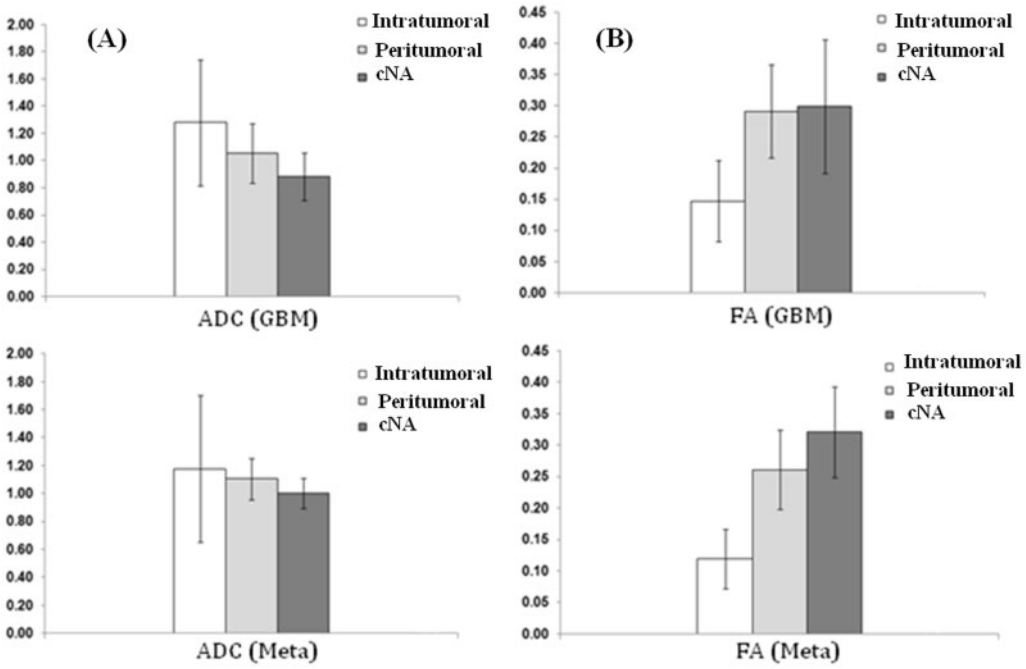

Figure 6 **Histograms illustrating a comparison of ADC (A) and FA (B) measurements in terms of the mean values with their corresponding standard deviation in the intratumoral region (upper row), peritumoral region (lower row) and the contralateral normal area (cNA) for glioblastomas (GBMs) and metastases (Meta).**

Peritumoral region

Based on the obtained diffusion measurements in the peritumoral area of GBMs and metastatic tumors, our initial hypothesis that there should be a distinct differentiation between the peritumoral regions of the two lesion types was not verified. Around metastases, ADC values were slightly increased compared with GBMs and the obtained FA values were relatively lower than GBMs, respectively; however, these differences failed to reach statistical significance. Hence, these results indicate that ADC and FA could not serve as differentiating diagnostic indices in the peritumoral region of GBMs and metastatic tumors.

Regarding ADC, previous studies have reported that ADC measurements around the lesions are not indicative and do not aid in the differentiation between them[24,38]. On the contrary, Lu et al. observed significantly higher ADC values around metastatic brain tumors compared with high-grade gliomas, while other studies have reported that diffusion around glioblastomas is increased (i.e., higher ADC) compared with metastases[18,21,25]. These findings might be explained by the nature of the surrounding edema, present both in glioblastomas and metastatic tumors, and their effect on the directionality of water diffusion.

Regarding FA, the values measured did not lead to a distinct differentiation; however, based only on the mean values and the corresponding SDs for both tumor groups (Fig. 6B), FA was higher around glioblastomas than metastases. Higher FA values around GBMs may be attributed to the increased cell density due to infiltrations in the peritumoral region adjacent to the tumor core of GBMs, which might cause water molecules to diffuse with a higher degree of directionality, in contrast to metastatic tumors that are in general non-infiltrating; hence fiber organization around these lesions is not disrupted. Nevertheless, even though hypothetically fractional anisotropy around metastases is expected to reach the normal values, in this study the mean FA value on the periphery of the metastatic lesions was relatively lower than on the contralateral normal side, suggesting that the increased water concentration in the surrounding vasogenic edema leads to a more disorganized diffusion (i.e., decreased FA). Previous studies have reported similar results, observing significantly lower FA values in the peritumoral region of metastatic tumors in comparison with high-grade gliomas[18].

In conclusion, the low differentiation ability in terms of diffusion anisotropy in the peritumoral region of the aforementioned tumor groups might indicate that the glioma-related FA changes induced by both increased water content and tumor cells are potentially comparable with the metastasis-related changes caused solely by the increased water content.

DSCE imaging

Increased rCBV was previously found in peritumoral edema of glioblastomas[47]. Supposing that peritumoral rCBV is not increased in metastases, we aimed to evaluate whether rCBV values of the intratumoral and

peritumoral areas could differentiate solitary metastasis from GBM.

Intratumoral region

In this study, the rCBV ratios obtained from the intratumoral region did not enable the differentiation of glioblastomas from metastases. The measured rCBV values were 11.49 ± 6.33 for glioblastomas and 10.80 ± 5.13 for metastatic tumors, and no statistical differentiation was achieved between the two tumor groups, which is in agreement with previous studies[1,8,48–52]. These findings may be attributed to the fact that these tumors present high vascularity, abnormal capillary permeability and breakdown of the blood–brain barrier, and consequently they demonstrate increased rCBV ratio values.

Peritumoral region

The mean rCBV ratio value within the peritumoral region in glioblastomas was 1.68 ± 0.59, higher than the corresponding rCBV value from the cNA (1.13 ± 0.36), which suggests increased peritumoral perfusion resulting from the increased microvascular density and diminished perfusion on distant areas. On the contrary, the peritumoral rCBV ratio of metastatic tumors (1.06 ± 0.38) did not statistically differ from the corresponding normal area (0.96 ± 0.19). It must be noted that there was a tendency toward higher rCBV ratio values of the considered normal areas in glioblastoma cases in comparison with metastases. In fact, neoplastic cells in some high-grade gliomas can be infiltrated, not only outside the contrast-enhancing tumor margin but also far beyond the outer edematous edge that is clearly visible on the T2-weighted images, and might be a possible explanation for the relatively higher mean rCBV ratio value in glioblastoma cases[48].

Our study demonstrates that the rCBV ratio from the peritumoral region of glioblastomas and intracranial metastases significantly differed ($P < 0.02$), in accordance with previous observations[1,8,47–49].

Pathophysiologic findings of the two entities confirm these results, since in metastatic tumors the peritumoral area represents pure vasogenic edema rich in proteins caused by increased plasma fluid leakage from capillaries in or around the metastases[48,48,53]. Thus, there is no histologic evidence of tumor beyond the outer contrast-enhancing margin of the tumor, and the peritumoral region represents the reaction of the surrounding edematous but intrinsically normal brain parenchyma[48]. Furthermore, as Hossman and Bloink stated, blood flow measurements in edematous tissue have shown to be decreased due to local compression of the microcirculation by edema[54]. The aforementioned factors may account for the significantly lower rCBV ratio of metastases in comparison with that of glioblastomas, as presented in this study.

On the other hand, in the peritumoral region of glioblastomas the vasculature is relatively impervious and the peritumoral T2-hyperintensity is a combination of tumor infiltration along the perivascular spaces and vasogenic edema, explaining the increased peritumoral rCBV ratio values[8,55].

In this particular study a cut-off value of 1.70 in the peritumoral rCBV ratio was calculated, which discloses a sensitivity of 80% and a specificity of 93.8% in the discrimination of these two tumor types. Although many DSCE MRI studies provide different cut-off values ranging from 0.8 to 1.8 to differentiate between GBMs and metastases, the reported levels of sensitivity and specificity remain quite similar[1,8,47–49,54,56–58].

It must be mentioned that a homogenized brain metastasis material would be the optimum in such types of study, as the nature of the primary tumor is very important in the differential diagnosis. Moreover, it should be expected that metastatic lesions originating from the same primary sites may potentially present similar diffusion, perfusion and metabolic characteristics, providing further discrimination among metastatic lesions per se.

Summary

Summarizing all the above results regarding the evaluation of MRSI, DWI, DTI and DSCE MRI in the differentiation of glioblastomas multiforme from solitary metastases, we conclude to the following:

Intratumoral region

None of the investigated MR techniques and their corresponding parameters was able to differentiate GBMs from metastatic tumors by evaluating the intratumoral part of the lesions.

Peritumoral region

Statistically significant differentiating indices

The metabolic ratios NAA/Cr, Cho/Cr and Cho/NAA obtained from MRS as well as the rCBV from DSCE MRI showed high differentiation ability between the two tumor groups, supporting the hypothesis that the peritumoral region of glioblastomas is characterized by extensive infiltration of tumor cells whereas the peritumoral region of metastases contains almost purely vasogenic edema.

Non-statistically significant differentiating indices

The diffusion parameters ADC and FA could not reach statistically significant differentiation between the two lesion types, most probably because of the nature of the surrounding edema, present both in glioblastomas

and metastatic tumors, and its controversial effect on the directionality of water diffusion.

Conclusion

Advanced MRI techniques are required in many clinical cases where conventional MRI fails to differentiate malignant lesions such as glioblastomas and metastases. ^{1}H-MRS, DWI, DTI and DSCE MRI has been incorporated in the clinical routine to improve specificity and provide an insight into the underlying biological characteristics of brain tumors.

In this study, we concluded that ADC and FA cannot be used with statistical certainty to significantly differentiate between glioblastomas and metastases, although there is a possibility that larger patient populations might validate a tendency for differentiation using the FA values peritumorally.

On the other hand, DSCE imaging and spectroscopic imaging measurements demonstrated significant differences, especially in the peritumoral region of solitary metastases and glioblastomas, so their use is strongly recommended in the differential diagnosis of these tumor entities.

References

[1] Chiang IC, Kuo YT, Lu CY, et al. Distinction between high-grade gliomas and solitary metastases using peritumoral 3-T magnetic resonance spectroscopy, diffusion, and perfusion imagings. Neuroradiology 2004; 46: 619–627. PMid:15243726.

[2] Hollingworth W, Medina LS, Lenkinski RE, et al. A systematic literature review of magnetic resonance spectroscopy for the characterization of brain tumors. AJNR Am J Neuroradiol 2006; 27: 1404–1411. PMid:16908548.

[3] Cha S, Pierce S, Knopp EA, et al. Dynamic contrast-enhanced T2*-weighted MR imaging of tumefactive demyelinating lesions. AJNR Am J Neuroradiol 2001; 22: 1109–1116. PMid:11415906.

[4] Warren KE. NMR spectroscopy and pediatric brain tumors. Oncologist 2004; 9: 312–318. doi:10.1634/theoncologist.9-3-312. PMid:15169986.

[5] Cha S. Neuroimaging in neuro-oncology. Neurotherapeutics 2009; 6: 465–477. doi:10.1016/j.nurt.2009.05.002. PMid:19560737.

[6] Toh CH, Castillo M, Wong AM, et al. Primary cerebral lymphoma and glioblastoma multiforme: differences in diffusion characteristics evaluated with diffusion tensor imaging. AJNR Am J Neuroradiol 2008; 29: 471–475. doi:10.3174/ajnr.A0872. PMid:18065516.

[7] Barker PB, Hearshen DO, Boska MD. Single-voxel proton MRS of the human brain at 1.5T and 3.0T. Magn Reson Med 2001; 45: 765–769. doi:10.1002/mrm.1104. PMid:11323802.

[8] Law M, Cha S, Knopp EA, et al. High-grade gliomas and solitary metastases: differentiation by using perfusion and proton spectroscopic MR imaging. Radiology 2002; 222: 715–721. doi:10.1148/radiol.2223010558. PMid:11867790.

[9] Howe FA, Barton SJ, Cudlip SA, et al. Metabolic profiles of human brain tumors using quantitative in vivo ^{1}H magnetic resonance spectroscopy. Magn Reson Med 2003; 49: 223–232. doi:10.1002/mrm.10367. PMid:12541241.

[10] Moller-Hartmann W, Herminghaus S, Krings T, et al. Clinical application of proton magnetic resonance spectroscopy in the diagnosis of intracranial mass lesions. Neuroradiology 2002; 44: 371–381. PMid:12012120.

[11] Fan G, Sun B, Wu Z, et al. In vivo single-voxel proton MR spectroscopy in the differentiation of high-grade gliomas and solitary metastases. Clin Radiol 2004; 59: 77–85. doi:10.1016/j.crad.2003.08.006. PMid:14697379.

[12] Bulakbasi N, Kocaoglu M, Ors F, et al. Combination of single-voxel proton MR spectroscopy and apparent diffusion coefficient calculation in the evaluation of common brain tumors. AJNR Am J Neuroradiol 2003; 24: 225–233. PMid:12591638.

[13] Chenevert TL, Brunberg JA, Pipe JG. Anisotropic diffusion in human white matter: demonstration with MR techniques in vivo. Radiology 1990; 177: 401–405. PMid:2217776.

[14] Doran M, Hajnal JV, Van Bruggen N, et al. Normal and abnormal white matter tracts shown by MR imaging using directional diffusion weighted sequences. J Comput Assist Tomogr 1990; 14: 865–873. doi:10.1097/00004728-199011000-00001. PMid:2229559.

[15] Hansen JR. Pulsed NMR study of water mobility in muscle and brain tissue. Biochim Biophys Acta 1971; 230: 482–486. doi:10.1016/0304-4165(71)90177-2. PMid:5581279.

[16] Liu X, Tian W, Kolar B, et al. MR diffusion tensor and perfusion-weighted imaging in preoperative grading of supratentorial nonenhancing gliomas. Neuro-Oncology 2011; 13: 447–455. doi:10.1093/neuonc/noq197. PMid:21297125.

[17] Chawla S, Zhang Y, Wang S, et al. Proton magnetic resonance spectroscopy in differentiating glioblastomas from primary cerebral lymphomas and brain metastases. J Comput Assist Tomogr 2010; 34: 836–841. doi:10.1097/RCT.0b013e3181ec554e. PMid:21084897.

[18] Lu S, Ahn D, Johnson G, et al. Peritumoral diffusion tensor imaging of high-grade gliomas and metastatic brain tumors. AJNR Am J Neuroradiol 2003; 24: 937–941. PMid:12748097.

[19] Morita K, Matsuzawa H, Fujii Y, et al. Diffusion tensor analysis of peritumoral edema using lambda chart analysis indicative of the heterogeneity of the microstructure within edema. J Neurosurg 2005; 102: 336–341. PMid:15739563.

[20] Oh J, Cha S, Aiken AH, et al. Quantitative apparent diffusion coefficients and T2 relaxation times in characterizing contrast enhancing brain tumors and regions of peritumoral edema. J Magn Reson Imaging 2005; 21: 701–708. doi:10.1002/jmri.20335. PMid:15906339.

[21] Pavlisa G, Rados M, Pavic L, et al. The differences of water diffusion between brain tissue infiltrated by tumor and peritumoral vasogenic edema. Clin Imaging 2009; 33: 96–101. doi:10.1016/j.clinimag.2008.06.035. PMid:19237051.

[22] Lee EJ, ter Brugge K, Mikulis D, et al. Diagnostic value of peritumoral minimum apparent diffusion coefficient for differentiation of glioblastoma multiforme from solitary metastatic lesions. AJR Am J Roentgenol 2011; 196: 71–76. doi:10.2214/AJR.10.4752. PMid:21178049.

[23] Yamasaki F, Kurisu K, Satoh K, et al. Apparent diffusion coefficient of human brain tumors at MR imaging. Radiology 2005; 235: 985–991. doi:10.1148/radiol.2353031338. PMid:15833979.

[24] Reiche W, Schuchardt V, Hagen T, et al. Differential diagnosis of intracranial ring enhancing cystic mass lesions–role of diffusion-weighted imaging (DWI) and diffusion-tensor imaging (DTI). Clin Neurol Neurosurg 2010; 112: 218–225. doi:10.1016/j.clineuro.2009.11.016. PMid:20053496.

[25] Lu S, Ahn D, Johnson G, et al. Diffusion-tensor MR imaging of intracranial neoplasia and associated peritumoral edema: introduction of the tumor infiltration index. Radiology 2004; 232: 221–228. doi:10.1148/radiol.2321030653. PMid:15220505.

[26] Krabbe K, Gideon P, Wagn P, et al. MR diffusion imaging of human intracranial tumours. Neuroradiology 1997; 39: 483–489. doi:10.1007/s002340050450. PMid:9258924.

[27] Bruhn H, Frahm J, Gyngell ML, et al. Noninvasive differentiation of tumors with use of localized H-1 MR spectroscopy in vivo: initial experience in patients with cerebral tumors. Radiology 1989; 172: 541–548. PMid:2748837.

[28] Server A, Josefsen R, Kulle B, et al. Proton magnetic resonance spectroscopy in the distinction of high-grade cerebral gliomas from single metastatic brain tumors. Acta Radiol 2010; 51: 316–325. doi:10.3109/02841850903482901. PMid:20092374.

[29] Ricci R, Bacci A, Tugnoli V, et al. Metabolic findings on 3T ^{1}H-MR spectroscopy in peritumoral brain edema. AJNR Am J Neuroradiol 2007; 28: 1287–1291. doi:10.3174/ajnr.A0564. PMid:17698529.

[30] Opstad KS, Murphy MM, Wilkins PR, et al. Differentiation of metastases from high-grade gliomas using short echo time ^{1}H spectroscopy. J Magn Reson Imaging 2004; 20: 187–192. doi:10.1002/jmri.20093. PMid:15269942.

[31] De Edelenyi FS, Rubin C, Esteve F, et al. A new approach for analyzing proton magnetic resonance spectroscopic images of brain tumors: nosologic images. Nat Med 2000; 6: 1287–1289. PMid:11062544.

[32] Preul MC, Caramanos Z, Collins DL, et al. Accurate, noninvasive diagnosis of human brain tumors by using proton magnetic resonance spectroscopy. Nat Med 1996; 2: 323–325. doi:10.1038/nm0396-323. PMid:8612232.

[33] Dowling C, Bollen AW, Noworolski SM, et al. Preoperative proton MR spectroscopic imaging of brain tumors: correlation with histopathologic analysis of resection specimens. AJNR Am J Neuroradiol 2001; 22: 604–612. PMid:11290466.

[34] Weber MA, Zoubaa S, Schlieter M, et al. Diagnostic performance of spectroscopic and perfusion MRI for distinction of brain tumors. Neurology 2006; 66: 1899–1906. doi:10.1212/01.wnl.0000219767.49705.9c. PMid:16801657.

[35] Chernov MF, Kubo O, Hayashi M, et al. Proton MRS of the peritumoral brain. J Neurol Sci 2005; 228: 137–142. doi:10.1016/j.jns.2004.11.039. PMid:15694194.

[36] Sinha S, Bastin ME, Whittle IR, et al. Diffusion tensor MR imaging of high-grade cerebral gliomas. AJNR Am J Neuroradiol 2002; 23: 520–527. PMid:11950638.

[37] Beppu T, Inoue T, Shibata Y, et al. Measurement of fractional anisotropy using diffusion tensor MRI in supratentorial astrocytic tumors. J Neurooncol 2003; 63: 109–116. doi:10.1023/A:1023977520909. PMid:12825815.

[38] Kono K, Inoue Y, Nakayama K, et al. The role of diffusion-weighted imaging in patients with brain tumors. AJNR Am J Neuroradiol 2001; 22: 1081–1088. PMid:11415902.

[39] Castillo M, Smith JK, Kwock L, et al. Apparent diffusion coefficients in the evaluation of high-grade cerebral gliomas. AJNR Am J Neuroradiol 2001; 22: 60–64. PMid:11158889.

[40] Provenzale JM, McGraw P, Mhatre P, et al. Peritumoral brain regions in gliomas and meningiomas: investigation with isotropic diffusion-weighted MR imaging and diffusion-tensor MR imaging. Radiology 2004; 232: 451–460. doi:10.1148/radiol.2322030959. PMid:15215555.

[41] Rees JH, Smirniotopoulos JG, Jones RV, et al. Glioblastoma multiforme: radiologic-pathologic correlation. Radiographics 1996; 16: 1413–1438; quiz 62–63. PMid:8946545.

[42] Altman DA, Atkinson DS, Jr. Brat DJ. Best cases from the AFIP: glioblastoma multiforme. Radiographics 2007; 27: 883–888. doi:10.1148/rg.273065138. PMid:17495298.

[43] Kinoshita M, Hashimoto N, Goto T, et al. Fractional anisotropy and tumor cell density of the tumor core show positive correlation in diffusion tensor magnetic resonance imaging of malignant brain tumors. Neuroimage 2008; 43: 29–35. doi:10.1016/j.neuroimage.2008.06.041. PMid:18672074.

[44] Beppu T, Inoue T, Shibata Y, et al. Fractional anisotropy value by diffusion tensor magnetic resonance imaging as a predictor of cell density and proliferation activity of glioblastomas. Surg Neurol 2005; 63: 56–61. doi:10.1016/j.surneu.2004.02.034. PMid:15639528.

[45] Stadlbauer A, Ganslandt O, Buslei R, et al. Gliomas: histopathologic evaluation of changes in directionality and magnitude of water diffusion at diffusion-tensor MR imaging. Radiology 2006; 240: 803–810. doi:10.1148/radiol.2403050937. PMid:16926329.

[46] Wang S, Kim S, Chawla S, et al. Differentiation between glioblastomas and solitary brain metastases using diffusion tensor imaging. Neuroimage 2009; 44: 653–660. doi:10.1016/j.neuroimage.2008.09.027. PMid:18951985.

[47] Blasel S, Jurcoane A, Franz K, et al. Elevated peritumoural rCBV values as a mean to differentiate metastases from high-grade gliomas. Acta Neurochir (Wien) 2010; 152: 1893–1899. doi:10.1007/s00701-010-0774-7.

[48] Cha S. Perfusion MR imaging of brain tumors. Top Magn Reson Imaging 2004; 15: 279–289. doi:10.1097/00002142-200410000-00002. PMid:15627003.

[49] Server A, Orheim TE, Graff BA, et al. Diagnostic examination performance by using microvascular leakage, cerebral blood volume, and blood flow derived from 3-T dynamic susceptibility-weighted contrast-enhanced perfusion MR imaging in the differentiation of glioblastoma multiforme and brain metastasis. Neuroradiology 2011; 53: 319–330. doi:10.1007/s00234-010-0740-3. PMid:20625709.

[50] Hakyemez B, Erdogan C, Gokalp G, et al. Solitary metastases and high-grade gliomas: radiological differentiation by morphometric analysis and perfusion-weighted MRI. Clin Radiol 2010; 65: 15–20. doi:10.1016/j.crad.2009.09.005. PMid:20103416.

[51] Cho SK, Na DG, Ryoo JW, et al. Perfusion MR imaging: clinical utility for the differential diagnosis of various brain tumors. Korean J Radiol 2002; 3: 171–179. doi:10.3348/kjr.2002.3.3.171. PMid:12271162.

[52] Preul C, Kuhn B, Lang EW, et al. Differentiation of cerebral tumors using multi-section echo planar MR perfusion imaging. Eur J Radiol 2003; 48: 244–251. doi:10.1016/S0720-048X(03)00050-0. PMid:14652141.

[53] Bertossi M, Virgintino D, Maiorano E, et al. Ultrastructural and morphometric investigation of human brain capillaries in normal and peritumoral tissues. Ultrastruct Pathol 1997; 21: 41–49. doi:10.3109/01913129709023246. PMid:9029765.

[54] Hossman KA, Bloink M. Blood flow and regulation of blood flow in experimental peritumoral edema. Stroke 1981; 12: 211–217. doi:10.1161/01.STR.12.2.211. PMid:7233466.

[55] Burger PC, Vogel FS, Green SB, et al. Glioblastoma multiforme and anaplastic astrocytoma. Pathologic criteria and prognostic implications. Cancer 1985; 56: 1106–1111. doi:10.1002/1097-0142(19850901)56:5<1106::AID-CNCR2820560525>3.0.CO;2-2. PMid:2990664.

[56] Bulakbasi N, Kocaoglu M, Farzaliyev A, et al. Assessment of diagnostic accuracy of perfusion MR imaging in primary and metastatic solitary malignant brain tumors. AJNR Am J Neuroradiol 2005; 26: 2187–2199. PMid:16219821.

[57] Calli C, Kitis O, Yunten N, et al. Perfusion and diffusion MR imaging in enhancing malignant cerebral tumors. Eur J Radiol 2006; 58: 394–403. doi:10.1016/j.ejrad.2005.12.032. PMid:16527438.

[58] Lehmann P, Saliou G, de Marco G, et al. Cerebral peritumoral oedema study: does a single dynamic MR sequence assessing perfusion and permeability can help to differentiate glioblastoma from metastasis? Eur J Radiol 2012; 81: 522–527. doi:10.1016/j.ejrad.2011.01.076. PMid:21334839.